RESEARCH ON OPTIMAL CONTROL ALGORITHM FOR POWER CHARACTERISTICS SEGMENTATION OF FORAGE HARVESTER
/
饲草收获机动力特性分割优化控制算法研究

Zheng WANG [1,2], Qingfu GONG [1], Fade LI [1], Ang GAO [1], Longlong REN [1], Yuepeng SONG[1,2,*]
[1] Shandong Agricultural University, College of Mechanical and Electrical Engineering/ China;
[2] Shandong Provincial Engineering Laboratory of Agricultural Equipment Intelligence/ China
E-mail: lntswangzheng@163.com
DOI: https://doi.org/10.35633/inmateh-69-02

Keywords: *Forage harvester; Dynamic allocation; Optimization control algorithm*

ABSTRACT
In order to improve the level of forage harvester automation and reduce damage, blockage and efficiency, based on the principle of minimum energy, fuzzy prediction theory and external characteristics of power, the mathematical model of the whole machine and each operating unit is established, and a set of forage harvester operating load adaptive feedback control system is designed; in order to make the power more scientifically and effectively distributed in real-time, the system adopts the simplified algorithm of operating unit efficacy threshold load splitting optimization control, with constant power and high efficiency. In order to make the power distribution more scientific and effective in real-time, the system adopts the simplified algorithm of operating unit efficacy threshold load splitting control to increase the load threshold of cutting and other operating units under constant power conditions, so that the operating efficiency of the whole machine can be improved. In the simulation test, the efficacy chopping load threshold ratio is about 1.08:1.01:1 for the three operation control methods of optimized control, fuzzy predictive control and PID control of the forage harvester, with 40% of the original feeding amount perturbation applied respectively, production efficiency was significantly improved.

摘要
为提高饲草收获机自动化作业水平和减损减堵提效，基于最小能量原理、模糊预测理论及动力外特性，建立整机及各作业单元的数学模型，并设计一套饲草收获机作业负荷自适应反馈控制系统：为使动力更加科学有效地实时分配，系统采用作业单元功效阈值负荷分割优化控制简化算法，恒动力条件下，提高切碎等作业单元的负荷阈值，从而使整机作业效能得到提升。仿真试验中，对饲草收获机的优化控制、模糊预测控制及 PID 控制三种作业控制方式，分别施加 40%的原喂入量扰动，功效切碎负荷阈值比约为 1.08:1.01:1。经现场试验，切碎负荷阈值比实际约为 1.078:1.004:1，该控制算法，使收获机的最大作业能力及其饲草生产效率都得到了明显提高。

INTRODUCTION

In recent years, many research attempts have been made at home and abroad to improve the automation and intelligence level of forage harvesters, select more appropriate feedback parameters, and innovate more advanced control algorithms to increase the efficiency and reduce the losses of forage harvesters, and great achievements have been made *(Chen et al., 2020; Chen et al., 2020; Li et al.2019)*.

Foreign scholar Jim Kruse used the engine load change to characterize the harvester load as a feedback parameter, and adjusted the walking speed of the whole machine in real time *(Jim,1983).* Kotyk et al. studied the load detection and feedback technology of the feeding amount of agricultural machinery, which reduced the operation power consumption and locked rotor failure rate, and improved the production efficiency *(Kotyk et al., 1991)*. Coen and others used fuzzy technology to build a control framework, and realized automatic operation of the combine based on model predictive control technology, reducing labour intensity *(Coen et al., 2006).* Baruah and others built the mathematical model of the whole machine based on the overall energy consumption *(Baruah et al., 2005)*; Reddy et al. fused explicit knowledge of design and implicit knowledge of design intent from the perspective of mechanical modeling technology of intelligent agricultural machinery to improve the flexibility, adaptability and reusability of the model *(Reddy et al., 2018)*.

Zheng Wang, Ph.D. Stud. Eng.; Qingfu Gong, M.Sc. Stud. Eng.; Fade Li, Prof. Ph.D. Eng.; Ang Gao, M.Sc. Stud. Eng.; Longlong Ren Lecturer Ph.D. Eng; Yuepeng Song, Prof. Ph.D. Eng.

Some students of China Agricultural University used digital modeling for high-end complex intelligent agricultural machinery and equipment to form a digital design technology system platform suitable for typical agricultural equipment products such as tractors and combine harvesters *(Du et al., 2019; Zhai et al., 2021).* Zhang Zhicheng et al. implemented intelligent control of work load based on fuzzy technology and variable quality working condition, proposed and implemented single-chip fuzzy control technology, which is not convenient for realizing strong nonlinear threshing drum of harvester when applied to traditional control theory automatic control of complex systems *(Zhang et al., 2001; Ji et al., 2008).* Li Guodong studies the constant speed of work based on pattern recognition technology, to further improve the robustness and discrimination of recognition. The low rank discriminant adaptive optimization algorithm is also proposed to solve the objective function and its effectiveness is verified *(Li et al., 2007)*. In addition, Ni Jun applied FPGA design speed fuzzy controller for specific real-time problems such as large inertia time delay *(Ni et al., 2009)*, and Qin Yun of Jiangsu University used neural network adaptive generalized predictive control technology to achieve control parameter output under different working conditions *(Zhao, 2009; Dong, 2010; Qi, 2012)*. However, they are often restricted by the level of software, hardware and other conditions. In terms of the specific application effect of the control algorithm for indicators such as steady-state accuracy, dynamic responsiveness and robustness, some studies can strengthen the characteristics of the controlled object, but are limited by the number of control parameters of the research object *(Yang, 2007)*; It ensures the dynamic stability output of the equipment, but the research on the time-delay control problem that may cause sudden changes in working conditions is relatively insufficient *(Rahman et al., 2020; Zakwan et al., 2021; Pan et al., 2010)*.

Therefore, the integration and optimization of control algorithms has gradually become a hot topic for many scholars at home and abroad. The literature *(EIOT Big Data Lab, 2018)* points out that optimization algorithms play an obvious role in the improvement of operation accuracy, energy saving etc., but the improvement of efficiency under the adaptivity and high computational difficulty needs to be researched and broken through.

On the basis of ensuring the effect of the above traditional control algorithm research and application, this paper establishes the mathematical model and control system design of the whole machine and each work unit, proposes and implements an optimal control algorithm for reasonably dividing the threshold load of work, that is, in the control process, the threshold load is divided into zero, the system output is efficiently transferred from any initial condition to another terminal condition in a limited time, and hierarchical closed-loop control is implemented (PID, Fuzzy and predictive, etc.). The system output controllability is enhanced, the operation threshold load is improved, and the operation is simplified and the output value is stable.

MATERIALS AND METHODS

Minimum power distribution model

Forage harvester

The structure of forage harvester test bench is shown in Figure 1.

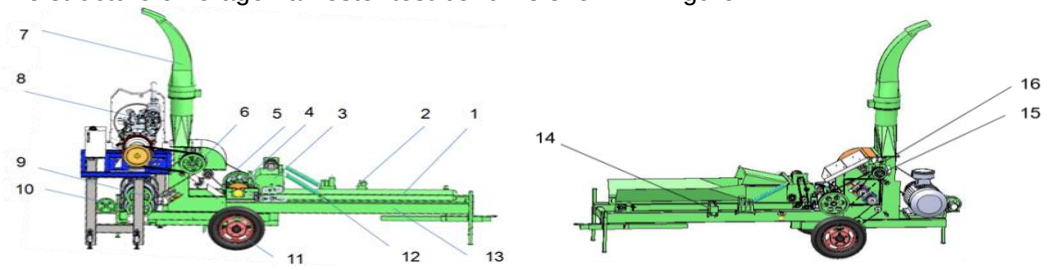

Fig. 1 - Forage harvester structure drawing
a) Right side of test bench; b) Left side of test bench

1. Feeding device; 2. Hydraulic signal proportional valve; 3. Cutting device; 4. Fixed knife and its regulating mechanism; 5. Grain crushing device; 6. Throwing mechanism; 7. Central tube bursting-type; 8. Diesel engine; 9. Motor; 10. Duplex hydraulic pump; 11. Traveling device; 12. Feed roll spring and tension sensor; 13. Frame; 14. Hydraulic flow signal proportional valve; 15. Speed Hall sensor; 16. Pressure sensor of drive belt

Table 1

Main operation technical parameters of forage harvester test bed

Project	Parameter
Length x Width x Height / mm	5454×2180×4319
Feeding system	belt
Feed inlet width / mm	535
Hobbing cutter rotation speed / $r \cdot min^{-1}$	1300
Feeding method	automatic straw feeder

Project	Parameter
Crop feeding per unit length kg / (m·s) Cutter roll type and specification Diameter x length / mm	5 Plate type drum cutter 476×560
Moving knife arrangement	"V" arrangement
Number of moving knives / piece Moving and fixed tool clearance / mm Slip cut angle / deg. Minimum working clearance of conditioner roll / mm	16 1 10° 1.5
Diesel engine power /kW	103.8
Rated speed / r·min^{-1}	2300
Maximum no-load speed / r·min^{-1}	2485±30
Idling / r·min-1	800±20
Maximum torque / N·m	562
Maximum torque speed / r·min^{-1}	1400～1800
Governor type	Whole process steel ball
Speed regulation range / r·min^{-1}	0～2300
Productivity /kg·h^{-1}	17×10^3（Fresh forage）

As shown in Figure 1, the forage harvester test-bed is mainly used for silage and yellow storage of forage. It can complete the feeding and conveying, chopping, crushing, throwing and loading of plants at one time. Its main operating loads and state quantities include feeding load, chopping roll speed, crushing roll speed, throwing fan speed, crop loss, crop height, etc. The operation characteristics of forage harvester (high-order nonlinearity, time variation, large inertia, pure time delay, parameter drift, asymmetry, etc.) are complex. In order to obtain better control effect, it is necessary to design and configure the automatic control system for the overall load of the harvester *(Ni et al., 2009)*, according to the actual working conditions reflected by the load data in the operation process, with the help of real-time optimal control of appropriate operation parameters. That is, the transmission belt pressure detection system detects the transmission belt load data in real time during the operation process, and timely feeds back the actual working conditions expressed by the data to the overall load of the harvester and the crop feeding control system. With the help of real-time control and adjustment of appropriate operating parameters, the control system realizes further automatic optimization and adjustment of the quality and efficiency of operations such as chopping, flattening and throwing, and reduces failures such as rotor blockage, wear and energy consumption, and ensure that the overall load of the harvester is in the best state for a long time *(Zhao, 2009)*. Table 1 shows the main operating parameters of the harvester. The rated productivity is 17×10^3 kg-h^{-1}, about 4.72 kg-s^{-1}. Since the cutting width of 535 mm is similar to the effective width of the chopping roller of 560 mm (feeding transverse length), the crop feeding volume per unit (cutting transverse) length was regularized to 5 kg/(m-s) in the field test.

The composition of main operation units of forage harvester is shown in Figure 2. The figure shows the specific installation and layout of the modules of each main operation unit of the forage harvester and the actual sample of the cutter roll of the shredding operation unit. The power transmission system structure of forage harvester is shown in Figure 3. The figure shows the power transmission system structure of the forage harvester, which is composed of belt transmission and hydraulic transmission.

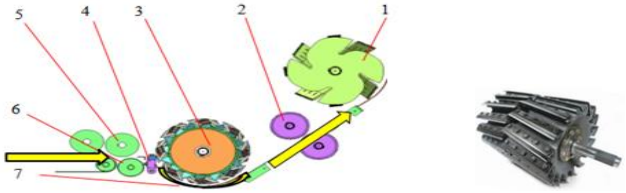

Fig. 2 - The main unit of work location and chopping unit diagram

1. Throwing device; 2. Grain crushing roller; 3. Chopping roller; 4. Fixed knife; 5. Upper feeding roller; 6. Lower feeding roller; 7. Chopping bottom arc plate

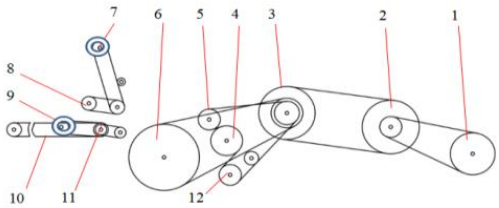

Fig. 3 - Schematic diagram on drive system for Forage Harvester

1. Hydraulic pump; 2. Engine pulley (largest); 3. Throwing device pulley (largest); 4. Lower grain crushing roller pulley; 5. Upper grain crushing roller pulley; 6. Chopper pulley; 7. Upper feed roller sprocket hydraulic motor; 8. Upper feed roller sprocket; 9. Lower feed roller sprocket hydraulic motor; 10. Conveyor belt; 11 Lower feed roller sprocket; 12. Tensioner wheel

The overall structure of the forage harvester operation load model is shown in Figure 4.

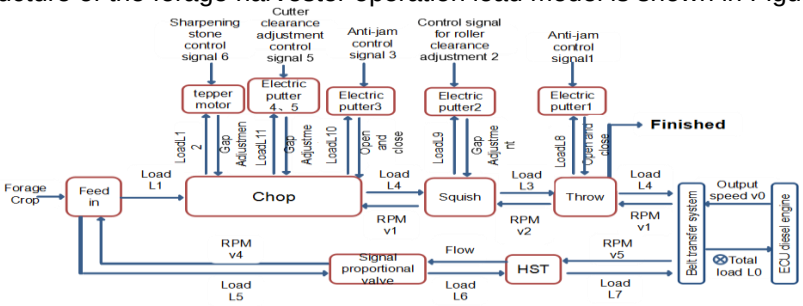

Fig. 4 - Load model structure of the forage crop harvester

Figure 4 shows that the main operating loads of the forage harvester test stand are, feeding load, chopping load, flattening load and throwing load, etc. The engine power is given to the main operating loads with reasonable algorithmic control distribution.

The functions of the control system are shown in Figure 5.

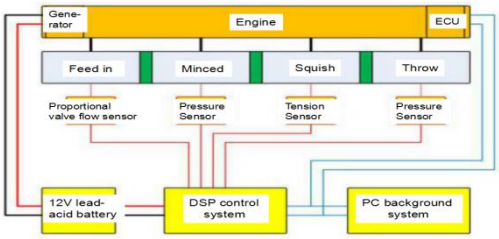

Fig. 5 - Functional Block Diagram on

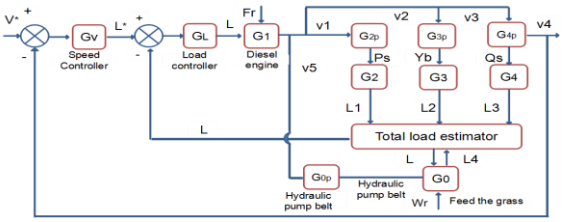

Fig. 6 - Forage harvester load control system structure drawing

The PID and other control systems of forage harvester operation are designed according to Fig. 5 and Fig. 6. The information of operating loads such as feeding, chopping, squashing and throwing are collected by the corresponding sensors and transmitted to the DSP information processing module of the main control board of the lower computer, and after the overall calculation, the control commands such as speed and torque are output to the engine through CAN bus to make the operating system run controllably in a stable and efficient way.

Minimum dynamic model and optimization objective

The power allocated to each operation unit in real time is the minimum, which can be equivalent to the minimum functional value of the objective function of the rotation angle and thrust of the main shaft of each operation unit of the harvester *(Gu et al., 2011)*. The objective function and constraint conditions of the rotation angle of the main shaft of the unit are:

$$J_{des} = \min\ J_i(\Delta\alpha, \Delta f, s) = \sum_{j=0}^{m}\left(\frac{dW_j}{df_j}(f_{0,j})\Delta f_j + \frac{d^2W_j}{df_j^2}(f_{0,j})\Delta f_j^2 + s^T Q s + \Delta\alpha^T \Omega \Delta\alpha\right) \quad (1)$$

The constraints are:

$$s.t. \quad s + B(\alpha_0)\Delta f + \frac{\partial}{\partial\alpha}(B(\alpha)f)\Big|_{\substack{\alpha=\alpha_0 \\ f=f_0}} \cdot \Delta\alpha = u - B(\alpha_0)f_0 \quad (2)$$

$$f_{min}/p - f_0 \le \Delta f \le f_{max}/p - f_0 \quad (3)$$

$$\alpha_{min} - \alpha_0 \le \Delta\alpha \le \alpha_{max} - \alpha_0$$

$$\Delta\alpha_{min} \le \Delta\alpha \le \Delta\alpha_{max}$$

where, J_i is the index value for the reduction of total power energy consumption of the unit; f_0 is the spindle thrust from the previous time's work unit; p is the force reduction factor *(Johansen et al., 2004)*; α is the spindle thrust angle; s is the spindle thrust error; The j operation period; m total of job periods; W is to minimize energy consumption; Q is the change rate of spindle thrust; Ω is the change rate of thrust azimuth angle of main shaft; u is the thrust command, and the first order inertia link of the low-pass filter is applied to it. Based on this objective function model, the dynamic and kinematic equations of each operation module and the whole machine of the equipment are established respectively.

The objective function and constraints of the spindle thrust of the work unit are:

$$\min\left\{J_i = f^T W f + s^T Q s\right\} \tag{4}$$

$$s.t. \quad B(\alpha) f = u + s \tag{5}$$

$$f_{\min} \le f \le f_{\max}$$

$$\Delta f_{\min} \le f - f_0 \le \Delta f_{\max}$$

Where, J_i is the optimal target value of the energy consumption reduction index of the work unit, f is the unit spindle thrust. Since the thrust azimuth of the main axis of the element $\alpha = \alpha_0 + \Delta\alpha$ can be calculated, the elements in the matrix $B(\alpha)$ are constant. In order to simplify the real-time calculation, u is a unit spindle thrust command with recursive relationship, so that the constraint conditions $B(\alpha) f = u + s$ are linear equations, which can avoid errors when the constraint conditions are linearized.

According to equations (2) and (5) below, the cutting operation unit of forage harvester is taken as the research object, and the control constraints of optimization algorithm are applied to the maximum value of real-time output of the cutting load division operation section, so as to reduce the load of the cutting operation system, reduce the energy consumption and locked rotor rate under the constant load, and finally improve the effective efficiency, where is the real-time load value of the operation; It is the load threshold of each divided operation segment. Therefore, it is proposed to optimize the control trajectory of the workload as shown in Figure 7.

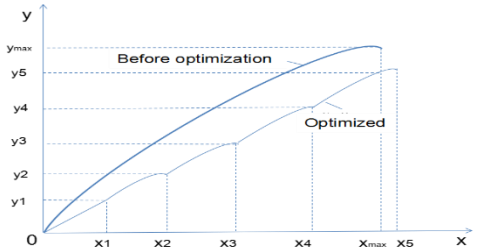

Fig. 7 - Schematic diagram of load control trajectory before and after optimization

In Figure 7, PID simplifies the design of the control system, and the traditional PID control algorithm expression is: $u(t) = K_p e(t) + K_i \int_0^t e(x)dx + K_d \frac{de(t)}{dt}$, where $u(t)$ is the output of the controller at t time, $e(t)$, $K_i \int_0^t e(x)dx$、$K_d \frac{de(t)}{dt}$ are the load control error, accumulation error and error change rate of the shredding and other operating units at time t respectively; K_p, K_i, K_d are the proportional, integral and differential parameters of PID control respectively. The fuzzy algorithm can enable the control system to define complex working conditions or have the strong robustness function of replanning definition and adaptation, and the predictive performance can eliminate the time delay in the operation process and save the system time to a certain extent. The above traditional algorithms adjust the control system according to deviation, deviation accumulation or deviation early warning value, and the internal constraints are small. Modern control is to adjust the performance of the system by entering and adjusting the characteristic values of the equation of state of the system, imposing constraints on both internal and external factors. The PID algorithm and fuzzy prediction algorithm with undivided task threshold load are pre-optimization algorithms. The fuzzy prediction algorithm of task threshold load segmentation is the optimization control algorithm of this study. The optimization control goal is that the load and energy consumption borne by the cutting knife with the same feeding amount at the same time are increased and reduced after optimization compared with before optimization.

Design of the chopping threshold load divider

Fitting and segmentation of engine external characteristic curve

The least square method is used to fit the fifth-degree polynomial of the dynamic characteristic curve, the equation derivation is used for quantitative prediction and segmentation, and the functional optimal trajectory algorithm is used.

The method steps are as follows:

Least square polynomial fitting equation of dynamic external characteristic curve. The least square fitting equation of engine speed torque external characteristic curve is obtained by Matlab:

$$\begin{cases} f(x) = 5.804\times10^{-13}x^5 - 4.378\times10^{-9}x^4 + 1.293\times10^{-5}x^3 - 0.019x^2 + 14.2x - 3874 \\ f'(x) = 2.902\times10^{-12}x^4 - 1.7512\times10^{-8}x^3 + 3.879\times10^{-5}x^2 - 0.038x + 14.2 \\ f''(x) = 1.1608\times10^{-11}x^3 - 5.2536\times10^{-8}x^2 + 7.758\times10^{-5}x - 0.038 \\ f'''(x) = 3.4824\times10^{-11}x^2 - 1.05072\times10^{-7}x + 7.758\times10^{-5} \end{cases} \quad (6)$$

Boundary value calculation and segmentation. Calculate the inflection point value of the above torque acceleration equation as the boundary value of the following functional prediction segmentation:

a. Boundary value calculation and segmentation

Calculate the inflection point value of the above torque acceleration equation as the boundary value of the following functional prediction segmentation:

The engine torque f value corresponding to the positive engine torque acceleration f ': (f 0 = 343.1, f '0=0); (f 1 =488.9, f '1=0); (f 2 = 497.3, f' 2=0.061); (f 3=507.8, f '3=0.122); (f 4 = 525.9, f '4 = 0.182); (f 5 = 562, f '5 = 0.182).

The engine torque f value corresponding to negative engine torque acceleration f' : (f 0 =562, f '0 = 0); (f 1 =561.6, f '1 = 0); (f 2 = 555.8, f' 2 = -0.102); (f 3 = 538.5, f '3= -0.203); (f 4 = 486.6, f '4 = -0.305); (f 5 =343.1, f '5 = -0.305).

Adopt the forecast segmentation method:

The engine torque f value corresponding to the positive engine torque acceleration f ': [343.1-525.9][0-0.182]; [488.9-525.9][0-0.182]; [497.3-525.9][0.061-0.182]; [507.8-525.9][0.122-0.182]; [525.9-525.9][0.182-0.182].

The engine torque f value corresponding to negative engine torque acceleration f ' : [525.9-437.5][-0.305-0]; [561.6-437.5][-0.305-0]; [555.8-437.5][-0.305--0.102]; [538.5-437.5][-0.305--0.203]; [486.6-437.5][-0.305--0.305].

Regularize the above segmentation into values in the interval [0,1] and [-1,0]:

Forward engine torque f and torque acceleration f ': (x1,x2)=[0,0]; [0.65, 0]; [0.93, 0]; [0.95, 0.33]; [0.97, 0.67]; [1, 1].

Negative engine torque f and torque acceleration f ': (x1,x2)=[0,0]; [0.20, 0]; [0.28, 0]; [0.27, -0.33]; [0.23, -0.67]; [0.11, -1]; [0, -1].

The power distributed to the shredder roll in real time is the minimum, which is converted into the minimum index function of the throttle thrust and angle of the diesel engine. The system state equation is set as: $\dot{x}_1(t)=x_2(t)$, $\dot{x}_2(t)=u(t)$; Boundary condition: the threshold load of shredding is measured through test, and it is also regular as 1 for convenience of programming and calculation; Initial state of engine torque *f* and torque acceleration *f'*: $[x_1(0), x_2(0)]$, final state $[x_1(t_r), x_2(t_r)]$.

b. Solution of optimal control trajectories of load functional

The fuzzy nonlinear predictive PID control with task threshold load segmentation is adopted. First, the shredding load algorithm is segmented and each boundary value is obtained. Then, the time-varying system is approximately simplified into a linear constant system through the generalized Lipschitz continuity condition (the minimum coefficient is taken in the test) and spline interpolation function applied in the prediction algorithm. Finally, the optimal control trajectory of each segment is solved using the minimum energy control principle. Construction of Hamiltonian function:

The control system is approximately a discrete steady system with fixed and free ends; According to equations (1), (2), (4) and (5), in order to avoid solving differential equations and singular structural terms, under the action of thrust reduction coefficient, p etc., to minimize the energy consumption, control constraints $|u(t)| \le 1$ are taken to determine the optimal control of all output solutions $u^*(t)$, and achieve the minimum energy performance index of equations (1) and (4). It can be equivalent to the shredding performance index:

$$J_{qdes} = \int_0^{tf} u^2(t)dt = \min$$

Sectional condition, boundary condition and law of variation H *(Hu,2007):*

$$x(t_0) = x_0,\ x(t_f) = x_f,\ \ H^*(t_f^*) = 0 \quad (7)$$

In order to turn the functional extremum with equality constraints into the functional extremum without constraints, according to formula (7), the Lagrangian multiplication operator is used to construct the Hamiltonian function $H(x, u, \lambda, t)=L(x, u, t)= \lambda^T(t)\, f(x, u, t)$, and the following results are obtained:

$$H = u^2 + \lambda_1 x_2 + \lambda_2 u = \left(u + \frac{1}{2}\lambda_2 \right)^2 + \lambda_1 x_2 - \frac{1}{4}\lambda_2{}^2 \tag{8}$$

which:

$$\begin{bmatrix} x_1 \\ x_2 \\ u \\ \lambda \end{bmatrix}(t) = \begin{bmatrix} \frac{1}{12}C_1 t^3 - \frac{1}{4}C_2 t^2 + C_3 t + C_4 \\ \frac{1}{4}C_1 t^2 - \frac{1}{2}C_2 t + C_3 \\ \frac{1}{2}(C_1 t - C_2) \\ -\frac{\partial H}{\partial x_1}, -\frac{\partial H}{\partial x_2} \end{bmatrix} \tag{9}$$

where, $x_1(t)$ is speed, $x_2(t)$ is torque, $u(t)$ is control quantity, $\lambda_i \in R^n$ is Lagrange multiplier vector, H is Hamiltonian function, and C_i is undetermined coefficient.

From the minimum condition:

$$u^*(t) = \begin{cases} +1, & \lambda_2(t) < -2 \\ -\frac{1}{2}\lambda_2(t), & |\lambda_2(t)| \le 2 \\ -1, & \lambda_2(t) > 2 \end{cases} \tag{10}$$

The optimal control is determined by the combination of the optimal trajectory change law and the final state conditions, so that the forage crops are fed from the known initial state, the equal quality processing is transferred to the control target set, and the fuel consumption is:

Forward sectional load: $J = -W(t_f) \to \min$

Segment I boundary conditions: $x_1(0)=0$, $x_2(0)=0$; $x_1(t_f)=1$, $x_2(t_f)=1$;

⋮ ⋮

Segment VI boundary conditions: $x_1(0)=0.97$, $x_2(0)=0.67$; $x_1(t_f)=1$, $x_2(t_f)=1$.

Load of each section in negative direction:

Segment I boundary conditions: $x_1(0)=0$, $x_2(0)=0$; $x_1(t_f)=0$, $x_2(t_f)=-1$;

⋮ ⋮

Segment VI boundary conditions: $x_1(0)=0.11$, $x_2(0)=-1$; $x_1(t_f)=0$, $x_2(t_f)=$-1.

After checking the $u(t_f)=\frac{1}{2}(C_1 t_f - C_2)$ of each segment, the conditions of $[0, t_f]$ and $|u(t)| \le 1$ are met in the $|\lambda_2(t)| \le 2$ segment, and $x_2^*(t) = \int u^*(t)\, dt$ is obtained for each segment; $x_1^*(t) = \int x_2^*(t)\, dt$ optimal control trajectory equation.

Application of splitter

The structure of the shredding threshold load undivided Kalman fuzzy nonlinear generalized predictive controller *(Fan et al., 2017)* is shown in Figure 8a. The structure of the chopped threshold load split Kalman fuzzy nonlinear generalized predictive controller is shown in Figure 8b. This structure is based on the former with an optimization control algorithm module.

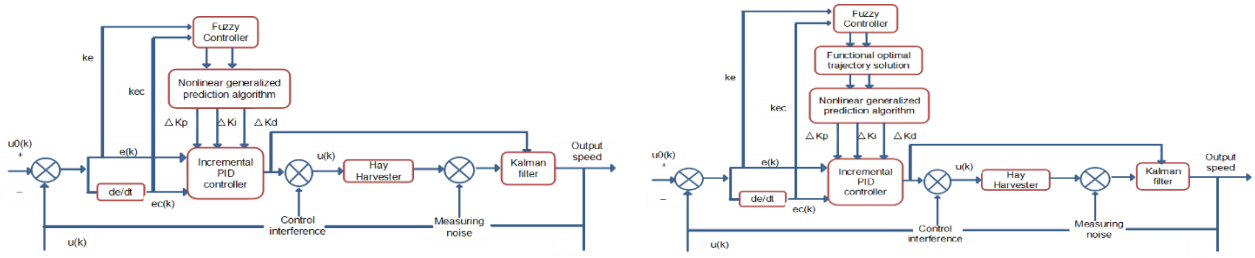

a Fuzzy Predictive PID Control Model b Fuzzy Predictive PID Optimal Control Model

Fig. 8 - Structure diagram of Emmerich Kálmán-fuzzy nonlinear generalized predictive controller

In the optimization control model, the shredding threshold load segmentation algorithm module is placed between the fuzzy algorithm module and the prediction algorithm module. After the fuzzy shredding load parameters are input. The output and prediction algorithm modules feedback control the shredding operation cycle. The function graph lines of each segment after segmentation are shown in Figure 9a, and the optimized trajectory graph lines in slope load control are shown in Figure 9b.

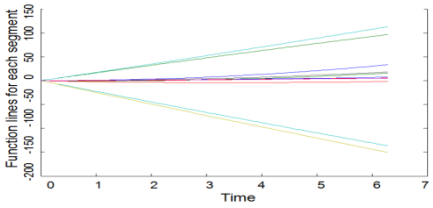

a Function lines of each segment after segmentation

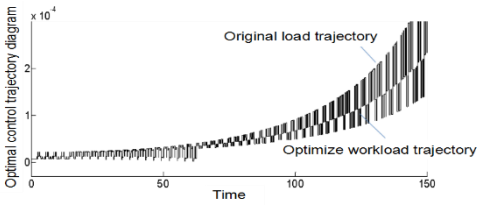

b Optimal trajectory in slope load control

Fig. 9 - Split diagram and control application diagram

Figure 9a shows the optimal control trajectories of each load segment based on the segmentation and minimum energy principle algorithm, and the linear segments with different approximate slopes. Figure 9b controls and adjusts a slope load simulation optimization algorithm with random input, and compares the graph and line conditions before and after the optimization control, showing the control adjustment of the same load at the same time, which is finally reduced compared with that before the optimization.

RESULTS

Simulation analysis

Under normal operation state, the simulation of steady state and disturbance transient response under PID control, fuzzy prediction (cutting threshold load is not divided) control, fuzzy prediction (cutting threshold load is divided) optimization control of forage harvester's cutting threshold load. After the normal operation is stable for a certain period of time, apply quantitative step and slope disturbance signals to the three working conditions respectively, detect the response of system parameters to the disturbance, and compare the operation effects before and after optimal control.

Steady state simulation of PID control, fuzzy predictive control and optimization control

The PID load feedback control system is used to control the cutting threshold load of the forage harvester. Under the condition of a certain amount of crop feed input, after a long enough time, the steady-state values of the engine, the feed roll and the cutting roll are detected, and the steady-state control results are obtained, as shown in Figure 10.

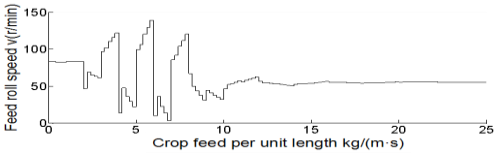

a) Rotation speed of closed-loop feeding roller and crop feeding amount

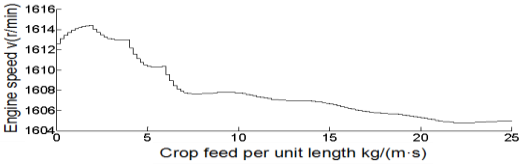

b) Closed loop engine speed and crop feed

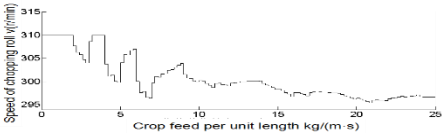

c) Rotation speed of closed loop chopper roll and crop feeding rate

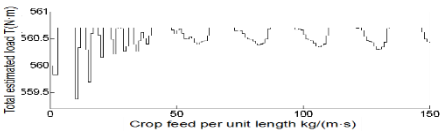

d) Closed loop population estimation load and crop feeding

Fig. 10 - Steady-state simulation diagram of closed-loop speed

The test results are shown in Figure 10. Engine: when the crop feeding amount is small, the controller automatically increases the speed of the chopping roll to obtain a larger feeding amount. When the crop feeding amount is less than 8 kg/(m▪s), the engine speed changes little. When the crop feeding amount exceeds 8 kg/(m▪s), the controller will gradually reduce the speed of the chopping roll, which will make the feeding amount tend to keep at the required level for operation. Feeding roller: the rotating speed is basically constant at about 55 r/min; The engine speed is still basically constant at about 1605 r/min; The speed of the chopping roll is basically constant at about 1295 r/min. Influenced by the real-time evaluation of the overall load estimator in the model, the feed roll speed, engine speed and chopping roll speed fluctuated during the stabilization process. See Table 2 for steady state deviation of feed roll, chopper roll and engine speed.

Table 2

Steady-state simulation deviation of operating unit speed for each model

Model type	Steady state deviation of feed roll speed (r/min)	Steady state deviation of chopping roll speed (r/min)	Steady state deviation of engine speed (r/min)
PID control	0.393	5.16	0.23
Fuzzy predictive control	0.340	3.70	0.25
Fuzzy predictive optimal control	0.300	4.33	0.07

The steady state deviation of the feed roll speed, the optimal control<fuzzy predictive control<PID control; Steady state deviation of chopping roll speed, fuzzy predictive control<optimal control<PID control; Steady state deviation of engine speed, optimal control<PID control<fuzzy predictive control. The steady-state error of the overall optimal control is the smallest, and the steady-state error of the PID control is the largest.

PID control, fuzzy predictive control and their optimal control Simulation of transient response to step disturbance:

Positive disturbance feeding: First, the harvester shall be at 5 kg/(m▪s). And then apply 2 kg/(m▪s) at 15 s. Feed loaded, test the transient response of the harvester engine speed, chopping speed and feed roll speed. Negative disturbance feeding: The harvester shall be at 7 kg/(m▪s) for stable operation under feeding of, subtract 2kg/(m▪s) feed load, test the transient response of the harvester engine speed, chopping speed and feed roll speed.

The simulation results are shown in Figure 11.

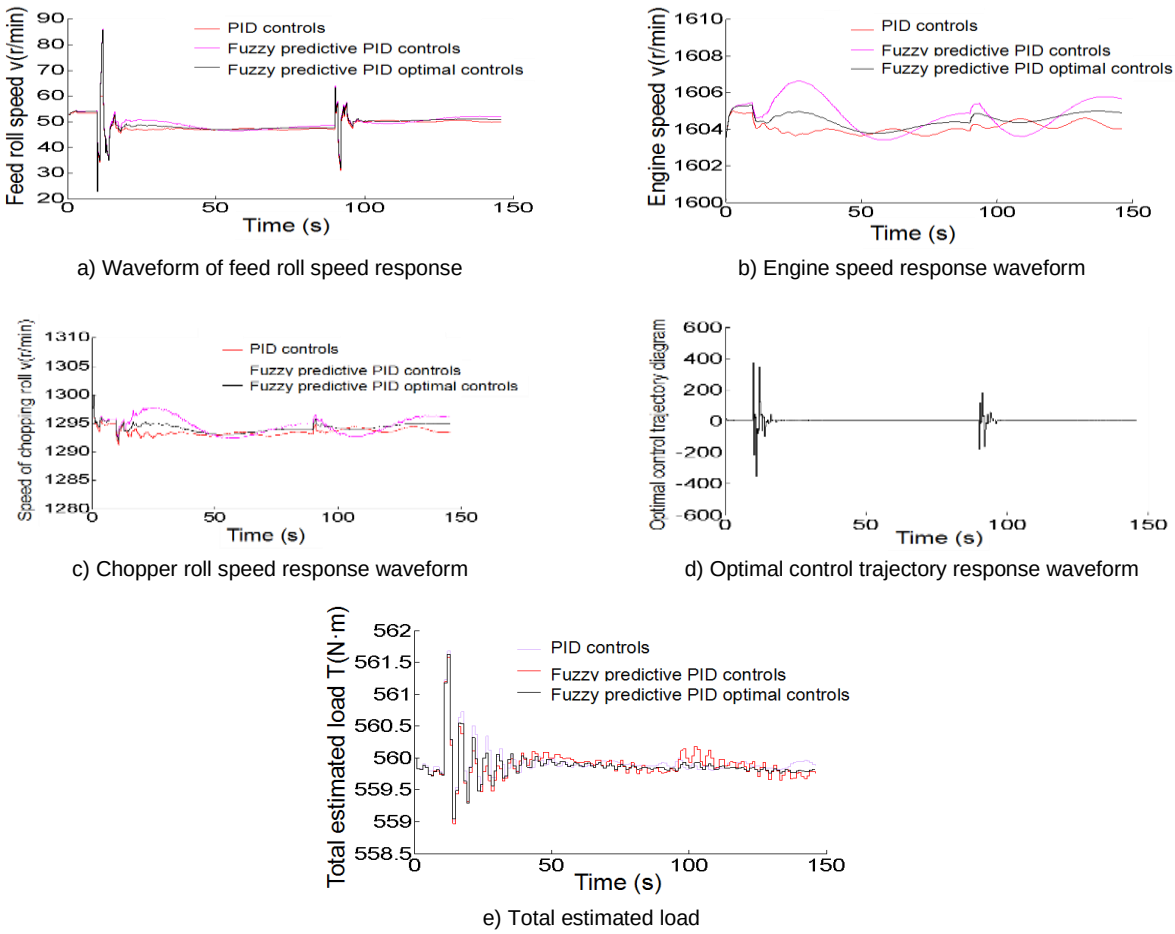

a) Waveform of feed roll speed response

b) Engine speed response waveform

c) Chopper roll speed response waveform

d) Optimal control trajectory response waveform

e) Total estimated load

Fig. 11 - Closed-loop simulation of step-positive and negative-disturbance transient response of crop feed per unit length

The torque corresponding to each speed is calculated according to equation (6), and the product of the load disturbance response time is obtained. The energy consumption of each model for load control is shown in Table 3.

Table 3

Speed and disturbance response time of model engines

Model type	Chopper roll disturbance speed (r/min)	Chopper roll disturbance torque (N·m)	Chopper roll disturbance response time (s)	Chopping energy consumption (10^4J)
PID control	1308.2	535.57	12.2	3.296
Fuzzy predictive control	1292.2	532.85	15.2	3.913
Fuzzy predictive optimal control	1292.4	532.89	11.0	2.575
Energy consumption comparison of shredding	Fuzzy predictive optimal control<PID control<fuzzy predictive control			

According to the disturbance simulation analysis of steady state and positive and negative feeding loads, in terms of improving the maximum operating capacity, the optimal control>PID control>fuzzy predictive control; For the response time of disturbance load, the optimal control<PID control<fuzzy predictive control; In terms of control robustness, optimal control<fuzzy predictive control<PID control; In terms of disturbance energy consumption, PID control is superior to fuzzy predictive control, and optimal control is superior to PID control. It can be seen that the optimization algorithm based on fuzzy predictive control plays an obvious role.

Test and result analysis

The test crop is corn straw, and the forage harvester test bench is first set at 2.5 kg/(m▪s). After stable operation for a period of time, increase to 5 kg/(m▪s), implement the feedback control of the forage harvester's operating load, and test the relationship between the steady state and transient responses of the harvester's engine speed, feed roll speed and the pressure load change of the chopping drive belt, as shown in Figure 12.

a) Quantitative weighing of corn straw

b) Quantitative feeding of corn straw

c) Chopping transmission belt pressure detection mechanism and optimal control of processed straw

Fig. 12 - Corn stalk chopping and other work load feedback control experiment

The initial design speed of the engine is 1000 r/min, the initial design pressure of the liquid suspension jacking roller of the chopping drive belt is 2.04 MPa, the input value of the chopping drive Belt pressure is 3.28 MPa, and the different PI controller parameter input values (K_p, K_i) of the control model in different time periods are shown in Table 4. The operation control verification of the pure mechanical operation, PID control, fuzzy predictive control, and fuzzy predictive optimization models is carried out.

Table 4

K_p and K_i input values for different time periods

Time	[0,18465]	[18466,35757]	[35758,47102]	[47103, 50268]
Control	Pure	PID control	Fuzzy predictive	Fuzzy predictive optimal
K_p, K_i	(0, 0)	(0.72, 0.23)	(0.58, 0.14)	(0.80, 0.26)

The speed disturbance response of the work unit under the control of each model on site is shown in Table 5, the steady state deviation of the speed of the work unit is shown in Table 6, the speed change and response time of the work unit are shown in Table 7, and the maximum disturbance tracking deviation of the speed of the work unit is shown in Table 8.

Table 5

Speed and disturbance response time of model engines

Control model	Feed roll speed (r/min)	Chopper roll speed (r/min)	Engine speed (r/min)
Pure machinery	54.77	798.2	911
PID control	54.83	708.0	906.5
Fuzzy predictive control	54.86	676.4	919
Fuzzy predictive optimal control	54.86	679.1	906

Table 6

Steady-state simulation deviation of operating unit speed for each model

Control model	Steady state deviation of feed roll speed (r/min)	Steady state deviation of chopping roll speed (r/min)	Steady state deviation of engine speed (r/min)
Pure machinery	1.368	24.0	8.05
PID control	0.668	26.5	14.22
Fuzzy predictive control	0.892	21.2	16.40
Fuzzy predictive optimal control	1.793	18.6	6.12

Table 5 and Table 6 show that the engine speed under optimal control is the lowest, and the steady state deviation of the shredding unit and the engine is the lowest.

Table 7

Simulation of operating unit speed change and response time disturbance under each model

Control model	Speed variation of feeding roller (r/min)	Chopper roll speed variation (r/min)	Engine speed variation (r/min)	Response time (s)
Pure machinery	2.28	67.0	17.1	195.7
PID control	6.62	73.4	17.6	172.1
Fuzzy predictive control	9.55	58.6	13.3	196.5
Fuzzy predictive optimal control	14.40	87.6	9.4	129.6

Table 8

Maximum disturbance tracking error for model units

Control model	Maximum disturbance tracking deviation of feed roll speed (r/min)	Maximum disturbance tracking deviation of chopper roll speed (r/min)	Maximum disturbance tracking deviation of engine speed (r/min)	The disturbance deviation of engine speed is more than the steady-state deviation (times)
Pure machinery	0.684	7.97	68.3	8.48
PID control	0.205	5.55	37.3	2.62
Fuzzy predictive control	1.792	10.72	23.5	1.43
Fuzzy predictive optimal control	0.915	13.34	46.3	7.56

According to Equation (6), the torque corresponding to the chopped disturbance speed and the energy consumption of each model for load control are shown in Table 9.

Table 9

Speed and disturbance response time of model engines

Control model	Minimum speed of chopping roll disturbance (r/min)	Chopper roll disturbance torque (N·m)	Chopper roll disturbance response time (s)	Chopping energy consumption (10^7J)
Pure machinery	728.6	272.3	195.7	1.453
PID control	634.6	139.8	172.1	1.490
Fuzzy predictive control	617.9	110.3	196.5	1.388
Fuzzy predictive optimal	591.5	59.7	129.6	1.382
Energy consumption comparison of shredding	Fuzzy predictive optimal control<fuzzy predictive control<pure machinery<PID control			

Finally, the comparison and analysis of energy efficiency between field operation disturbance control and simulation of each model are shown in Table 10.

Table 10

Comparison of model control performance

Test method		Step simulation	Practical Operation
Feed roll speed (r/min)		v2≈v3≈v4	v1≈v2≈v3≈v4
engine speed (r/min)		v2<v4<v3	v4<v3<v2<v1
Chopper roll speed (r/min)		v2<v3<v4	v4<v3<v2<v1
Steady state accuracy of operation (r/min)		μ4>μ3>μ2	μ4>μ3>μ1>μ2
Operation disturbance accuracy (r/min)		μ3>μ2>μ4	μ2>μ1>μ3>μ4
Response time of operation disturbance (s)		t4<t2<t3	t4<t2<t1<t3
Feeding tension load (MPa)		F3<F2<F4	F1<F2<F3<F4
Energy consumption of feeding roller (J)		Q4>Q2>Q3	Q4>Q3>Q2>Q1
Maximum pressure value of chopping drive belt (MPa)		P3<P2<P4	P2<P1<P3<P4
Average pressure value of chopping drive belt (MPa)		p4<p2<p3	p4<p3<p1<P2
Energy consumption of shredding roll (J)	Short operation time	Q4<Q2<Q3	Q4<Q2<Q3<Q1
	Operation duration		Q4<Q3<Q2<Q1
Maximum operation capacity (N)		N3<N2<N4	N2<N1<N3<N4
Production efficiency (%)		M3<M2<M4	M2<M1<M3<M4
Overall energy consumption (J)		Q4<Q2<Q3	Q4<Q3<Q1<Q2

Note: 1 - pure machinery; 2-PID control; 3 - Fuzzy measurement control; 4-Fuzzy predictive optimal control

From the above analysis, it can be seen that the trend of field test and step disturbance simulation results is basically the same. Under the same conditions of other input parameters of each model, when optimizing control, the maximum value of the pressure of the chopping drive belt increases, which increases the chopping threshold load. The overall performance of the optimization control system is a good control performance with the highest efficiency, the lowest energy consumption and the shortest disturbance response time. The experimental results were in line with the characteristics of optimal control effect and the processing quality of corn straw was good. However, it was also found in the study that the simulation results in Table 3 showed that the optimized control obtained fuel savings of about 21.9% compared to the traditional PID control, which theoretically exceeded the 18% already achieved in the actual production of John Deere 8000 series silage harvesters (*Wu, 2021*) and 10.6% of CLAAS JAGUAR 800 series silage harvesters (*Li, 2021*).

However, the field test results in Table 9 showed that the actual fuel savings obtained from the optimized algorithm control alone are about 7.2% compared to the conventional PID control and only about 4.9% compared to the pure mechanical operation, both of which are still far less than 18%, indicating that other aspects of forage harvester research need to be continuously optimized in parallel with this.

Through the above research, it is concluded that: 1) optimal control is the largest and PID control is the smallest in terms of maximum operation capacity. 2) In terms of control robustness, the operation time is longer, the PID control is lower than the fuzzy predictive control, the operation time is shorter, and the fuzzy predictive control is lower than the PID control; The optimal control combines the advantages of PID control and fuzzy predictive control, and has strong adaptability to the changes of operating load parameters, the fastest disturbance response, and the best robustness. It tends to be suitable for the control characteristics of long-term and continuous uncertain load operations. 3) In terms of control accuracy, crops are subject to sudden change feeding operation for a long time, and the disturbance accuracy of fuzzy predictive control is better than that of PID control. For short-term slope feeding operation, the disturbance accuracy of PID control is better than that of fuzzy predictive control. The disturbance accuracy of optimal control still needs to be further studied and improved. 4) In terms of overall energy efficiency, the optimal control of the shredding unit operation has realized greater operational capacity (threshold load) of the forage harvester, higher production efficiency and less total energy consumption per unit operation.

CONCLUSIONS

An optimal control algorithm for reasonably dividing the task threshold load, that is, in the control process, the threshold load is divided into parts, the system output is efficiently transferred from any initial condition to another terminal condition in a limited time, and hierarchical closed-loop control is implemented so that the system output controllability is enhanced, the task threshold load is improved, and the operation is simplified and the output value is stable.

The simulation results of PID control, fuzzy predictive control, and fuzzy predictive optimal control system show that the system disturbance responsiveness and energy efficiency are better than those of PID control and fuzzy predictive control. The optimal control algorithm can improve the maximum operating capacity of the forage harvester again based on the original control effect.

Finally, the above algorithms were applied to the forage harvester workload optimization feedback control operating system, which to some extent made up for the shortage of simply relying on traditional algorithms to control the workload, and realized the timely and reasonable supply of power required by the operation units such as shredding. Through the on-site actual machine test, the maximum operating capacity of the equipment was significantly improved.

ACKNOWLEDGEMENT

This work was sponsored by National key research and development "13th Five Year Plan" project (2016YFD0701701); Shandong modern agricultural industrial technology system - special fund for fruit innovation team (SDAIT-06-12) - special fund for fruit facilities, machinery and equipment post.

REFERENCES

[1] Baruah, D. C., Panesar, B.S., (2005). Energy requirement model for a combine harvester, part I: development of component models. *Biosystems Engineering,* Vol. 90, pp. 9-25, India.

[2] Chen, G., Wen, J., Zhang, R., Pan, C., Zhao Y., (2020). Advances and progress of agricultural machinery and sensing technology fusion (农业机械与信息技术融合发展现状与方向). *Smart Agriculture*, Vol. 2, pp. 1-16, Xinjiang/China.

[3] Chen, L., (2020). Evaluation of the standard timeliness of agricultural machinery standard citation network (农业机械标准引用网络的标准时效性评价). *Zhongnan University of Economics and Law*, DOI:10.27660/d.cnki.gzczu.2020.000010, Hubei/China.

[4] Coen, T., Paduart, J., Anthonis, J., (2006). Nonlinear system identification on a combine Harvester. *Proceedings of the 2006 American Control Conference*, pp. 3074-3079, USA.

[5] Du, F., Fu, H., Mao, R., Zhu, X., Li, Z., (2019). Development situation and prospects of intelligent design for agricultural machinery (农业机械智能化设计技术发展现状与展望). *Transactions of the Chinese Society for Agricultural Machinery*, Vol. 50, pp.1-17, Beijing/China.

[6] Dong, Q., (2010). Development of load feedback equipment of combine harvester based on gray predictive fuzzy control (基于灰色预测模糊控制的联合收割机负荷反馈装置的研制). *Jiangsu University*, Jiangsu/China.

[7] Fan, J., Wang, Z., Zhang, H., Zhao, Y., Song, P., (2017). Design and experiment of automatic levelling control system for orchards lifting platform (果园升降平台自动调平控制系统设计与试验). *Transactions of the Chinese Society of Agricultural Engineering*, Vol. 33, pp. 38-46, Shandong/China.

[8] Gu N., Miu M., Kuang F., (2011). A new allocation method for dynamic positioning systems (一种新的动力定位系统推力分配算法). *China offshore platform*, Vol. 26, pp. 50-52, Jiangsu/China.

[9] Hu, T., (2007). Automatic control theory (自动控制原理). *Beijing:* Science *press*, pp.553-557, Jiangsu/China.

[10] Ji, T., Wang, X., Fu, J., (2008). Grey prediction fuzzy PID control of the feeding quantity in combine (联合收获机喂入量灰色预测模糊 PID 控制). *Transactions of the Chinese Society for Agricultural Machinery*, Vol. 39, pp. 63-66, Henan/China.

[11] Johansen, T. A., Fossen, T. I., Berge, S. P., (2004). Constraint nonlinear control allocation with singularity avoidance using sequential quadratic programming. *IEEE Transactions on Control Systems Technology*, Vol. 12, pp. 211-216, Norway.

[12] Kotyk, W.H., Kirk, T.G., Klassen, N.D., (1991). Control system for combine harvesters. *WESCAN,* pp.96-102, USA.

[13] Kruse, J., (1983). Computer controls for the combine. *Agricultural Engineering*, Vol. 64, pp. 7-9, USA.

[14] Li, H., (2019). Development and application prospect on self-propelled whole-plant feeding forage Harvester (自走式全株喂入青饲料收获机的研制及推广应用前景). *Hebei Agricultural Machinery*, pp. 27, Hebei/China.

[15] Li, D., Han, C, Sang, Z., (2007). Design of Intelligent Controller of Constant Pal stance of Cylinder of the Combine (联合收割机脱粒滚筒恒速智能控制器设计). *Control Engineering of China*, Vol. 14, pp. 154-156, Gansu/China.

[16] Liu, J.N., (2019). Innovative Technology of CLAAS harvester. *Journal of Agricultural Engineering*, Vol.9(08), pp. 18-21, Beijing/China.
[17] Muhammad, Z., Saeed A., (2021). Distributed output feedback control of decomposable LPV systems with delay and switching topology: application to consensus problem in multi-agent systems. *International Journal of Control*, Vol. 94, pp. 2428-2439, Turkey.
[18] Ni, J., Mao, P., Cheng, H., (2009). Fuzzy control system of combine cylinder based on FPGA (基于FPGA 的联合收获机脱粒滚筒模糊控制系统).*Transactions of the Chinese Society for Agricultural Machinery*, Vol. 40, pp. 83-87, Jiangsu/China.
[19] Pan, J., Shao, T., Wang, K., (2010). Detection method on feed density for rice combine (水稻联合收割机喂入密度检测方法). *Transactions of the Chinese Society of Agricultural Engineering*, Vol. 26, pp. 113-116, Anhui/China.
[20] Qin, Y., (2012). Study on load control system of combined harvester (联合收割机负荷控制系统研究). *Jiangsu University*, Jiangsu/China.
[21] Reddy, E.J., Rangadu, V.P., (2018). Development of knowledge based parametric CAD modeling system for spur gear: an approach. *Alexandria Engineering Journa*l, Vol. 57, pp. 3139-3149, India.
[22] Sayedur, Rahman, S.M., Diponkar, P., Masud, R.M., (2020). Performance evaluation & operation of DSP control UPS system. *Engineering*, Vol. 12, pp. 666-681, Bangladesh.
[23] Wu, G., (2017). Big Mac Silage Harvester, the Big Guy has the big brain (巨无霸青贮收获机,大块头有大智慧). Farm Machinery, pp. 39-41, DOI:10.16167/j.cnki.1000-9868, Beijing/China.
[24] Xiang, W.H, Ban, L.G, Zhou, P.P., (2021). Online prediction and optimal control method of wind power sub-synchronous oscillation based on machine learning interpretable agent model (基于机器学习可解释代理模型的风电次同步振荡在线预测及优化控制方法). *Power system protection and control*, Vol. 49 (16), pp. 67-75, Beijing/China.
[25] Yang, L., (2007). Research on underwater image segmentation and recognition algorithm based on fractal theory (基于分形理论的水下图像分割与识别算法研究). *Huazhong University of Science and Technology*, Hubei/China.
[26] Zhai, Q., Wang, Q., Wang, L., Zhu, X., Du, F., Mao, R., (2021). Collaborative path planning for autonomous agricultural machinery of master-slave cooperation (面向主从跟随协同作业的导航路径规划方法). *Transactions of the Chinese Society for Agricultural Machinery,* Vol. 52, pp. 542-547, Beijing/China.
[27] Zhang, C., Sang, Z., (2001). Simulation research on the fuzzy logic control of an axial threshing cylinder (轴流脱粒滚筒模糊控制仿真). *Transactions of the Chinese Society for Agricultural Machinery*, Vol. 32, pp. 45-48, Anhui/China.
[28] Zhao, B., (2009). Intelligent control system research of combine load feedback (联合收割机负荷反馈智能控制系统的研究). Jiangsu University, Jiangsu/China.